AD-A038 665 BROWN UNIV PROVIDENCE R I DEPT OF CHEMISTRY F/G 7/4
FAR INFRARED STUDY OF CATION MOTION IN DRY AND SOLVATED MONO- A--ETC(U)
MAR 77 W M BUTLER, C L ANGELL, W MCALLISTER N00014-75-C-0883
UNCLASSIFIED TR-77-02 NL

1 OF 1
AD A038665

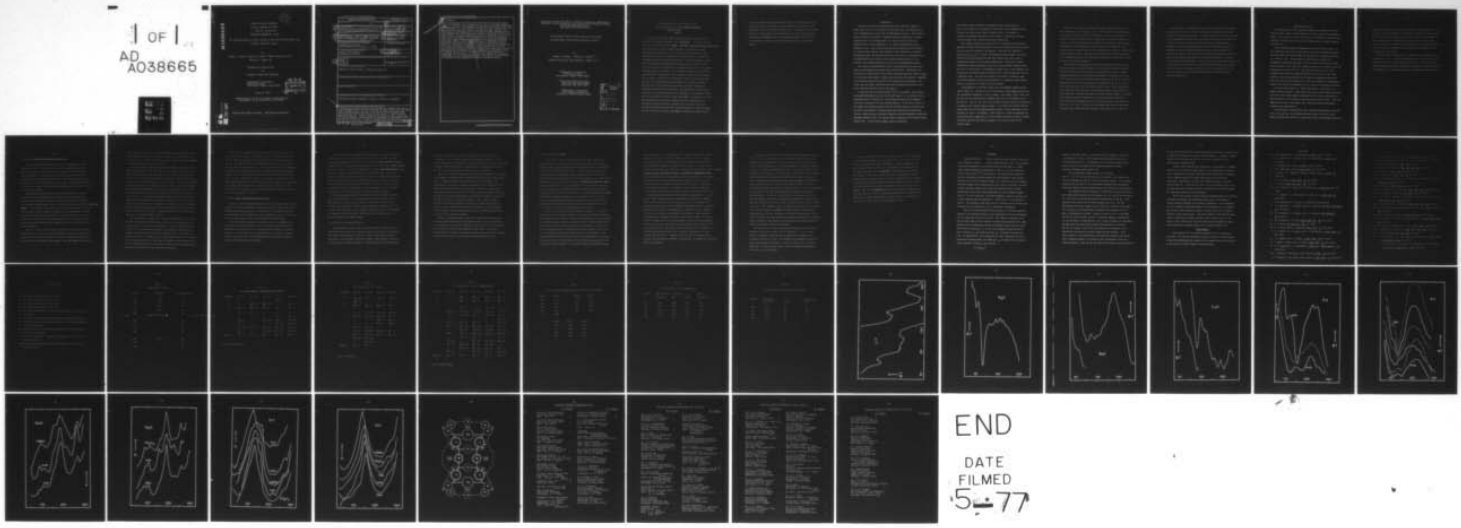

END
DATE FILMED
5-77

OFFICE OF NAVAL RESEARCH

Contract NOOO14-75-C-0883

Task No. NR 051-539

TECHNICAL REPORT NO. 77-02

Far Infrared Study of Cation Motion in Dry and Solvated Mono- and Divalent Zeolites X and Y

by

Wayne M. Butler, Charles L. Angell, Warren McAllister and

William M. Risen, Jr.

Prepared for Publication

in

Journal of Physical Chemistry

Department of Chemistry
Brown University
Providence, Rhode Island 02912

March 10, 1977

SECURITY CLASSIFICATION OF THIS PAGE (When Data Entered)

REPORT DOCUMENTATION PAGE	READ INSTRUCTIONS BEFORE COMPLETING FORM
1. REPORT NUMBER	2. GOVT ACCESSION NO. / 3. RECIPIENT'S CATALOG NUMBER
4. TITLE (and Subtitle): Far Infrared Study of Cation Motion in Dry and Solvated Mono- and Divalent Zeolites X and Y.	5. TYPE OF REPORT & PERIOD COVERED: Technical Report, 1977
	6. PERFORMING ORG. REPORT NUMBER: TR-77-02
7. AUTHOR(s): Wayne M. Butler, Charles L. Angell, Warren McAllister and William M. Risen, Jr.	8. CONTRACT OR GRANT NUMBER(s): N 000 14-75-C-0883 NR 051-539
9. PERFORMING ORGANIZATION NAME AND ADDRESS: Department of Chemistry Brown University, Providence, R. I. 02912	10. PROGRAM ELEMENT, PROJECT, TASK AREA & WORK UNIT NUMBERS
11. CONTROLLING OFFICE NAME AND ADDRESS: Office of Naval Research Department of the Navy	12. REPORT DATE: 10 March 1977
	13. NUMBER OF PAGES: 43
14. MONITORING AGENCY NAME & ADDRESS(if different from Controlling Office): 45p.	15. SECURITY CLASS. (of this report)
	15a. DECLASSIFICATION/DOWNGRADING SCHEDULE

16. DISTRIBUTION STATEMENT (of this Report)

Approved for Public Release: Distribution Unlimited

17. DISTRIBUTION STATEMENT (of the abstract entered in Block 20, if different from Report)

18. SUPPLEMENTARY NOTES

19. KEY WORDS (Continue on reverse side if necessary and identify by block number)

Ion Motion, zeolites, solvation, X zeolite, Y zeolite, far infrared

20. ABSTRACT (Continue on reverse side if necessary and identify by block number)

Far infrared ion motion bands have been observed and assigned in the spectra of dry synthetic zeolites X and Y containing Li^+, Na^+, K^+, Rb^+, Cs^+, Ag^+, Ca^{2+}, Sr^{2+}, and Ba^{2+} cations. The site I' and site II cation vibrational bands overlap and form the strongest feature in the spectra of samples exchanged with monovalent ions. The site I cation band appears at lower frequency than the site II envelope in these samples, but in divalent ion exchanged zeolites the opposite order occurs. A very low frequency site III cation band,

DD FORM 1 JAN 73 1473 EDITION OF 1 NOV 65 IS OBSOLETE
S/N 0102-014-6601 |

405 436

SECURITY CLASSIFICATION OF THIS PAGE (When Data Entered)

20. Continued

typical of monovalent X zeolites, has been observed in CsY. For a given cation, the frequency on X is higher than on Y due to the higher framework charge of X zeolites. The vibrational frequencies also follow an approximate $m^{-1/2}$ dependence for the two types of cation and the two forms of the zeolite. Solvation of the monovalent zeolites with H_2O, THF, DMSO, pyridine, and CH_2Cl_2 results in the appearance of a new band at higher frequency than the ion-framework modes which concurrently diminish in intensity, especially the site III band. The high frequency band is due to ion motion in a solvation shell which is unsymmetric at low hydration levels and at all solvation levels with organic adsorbates. In addition to a cation mass dependence, the ion-solvent frequencies are also dependent on the adsorbent's effective dielectric constant which is greater in X than Y. Increasing solvation shifts the ion-framework vibrations to lower frequency, but this shift with the organic adsorbates is primarily an indirect effect due to solvent delocalizing the framework charge. The implications of the cation vibrational frequencies for the mechanism of ionic conduction are considered in terms of a simple free-ion model. Ion transport in Y zeolites which have a large number of vacant cation sites so that each jump may be considered an independent event is adequately explained by this model, but ion transport in X zeolites is best interpreted in terms of cooperative effects.

Contribution from the Metcalf Research Laboratory, Department of Chemistry, Brown University, and the Tarrytown Technical Center, Union Carbide Corporation, and East Carolina University

Far Infrared Study of Cation Motion in Dry and Solvated Mono- and Divalent Zeolites X and Y

by

Wayne M. Butler,[1] Charles L. Angell,[2]

Warren McAllister[3] and William M. Risen, Jr.[1]

[1]Department of Chemistry
Brown University
Providence, Rhode Island 02912

[2]Tarrytown Technical Center
Union Carbide Corporation
Tarrytown, New York 10591

[3]Department of Chemistry
East Carolina University
Greenville, North Carolina 27834

Far Infrared Study of Cation Motion in Dry
and Solvated Mono- and Divalent Cation Containing
Zeolites X and Y

ABSTRACT

Far infrared ion motion bands have been observed and assigned in the spectra of dry synthetic zeolites X and Y containing Li^+, Na^+, K^+, Rb^+, Cs^+, Ag^+, Ca^{2+}, Sr^{2+}, and Ba^{2+} cations. The site I' and site II cation vibrational bands overlap and form the strongest feature in the spectra of samples exchanged with monovalent ions. The site I cation band appears at lower frequency than the site II envelope in these samples, but in divalent ion exchanged zeolites the opposite order occurs. A very low frequency site III cation band, typical of monovalent X zeolites, has been observed in CsY. For a given cation, the frequency on X is higher than on Y due to the higher framework charge of X zeolites. The vibrational frequencies also follow an approximate $m^{-1/2}$ dependence for the two types of cation and the two forms of the zeolite. Solvation of the monovalent zeolites with H_2O, THF, DMSO, pyridine, and CH_2Cl_2 results in the appearance of a new band at higher frequency than the ion-framework modes which concurrently diminish in intensity, especially the site III band. The high frequency band is due to ion motion in a solvation shell which is unsymmetric at low hydration levels and at all solvation levels with organic adsorbates. In addition to a cation mass dependence, the ion-solvent frequencies are also dependent on the adsorbent's effective dielectric constant which is greater in X than Y. Increasing solvation shifts the ion-framework vibrations to lower frequency, but this shift with the organic adsorbates is primarily an indirect effect

due to solvent delocalizing the framework charge. The implications of the cation vibrational frequencies for the mechanism of ionic conduction are considered in terms of a simple free-ion model. Ion transport in Y zeolites which have a large number of vacant cation sites so that each jump may be considered an independent event is adequately explained by this model, but ion transport in X zeolites is best interpreted in terms of cooperative effects.

INTRODUCTION

Molecular sieve zeolite structures have been intensively studied in recent years not only to relate pore size and molecular sieve behavior, but also to determine the active sites in heterogeneous catalysis. The catalytic sites fall into three classes: framework hydroxyl groups acting as either Bronsted acids (1) or Bronsted bases (2), Lewis acid sites within the framework such as three coordinate Al (3), and the exchangeable cations themselves (4,5). Since hydroxylated zeolites originate upon the hydrolysis of cations of high electric field strength or the deammination of ammonium exchanged zeolites, and since the Lewis acid sites occur in conjunction with the hydroxylated sites and more so upon thermal dehydroxylation (6) the catalytic site problem resolves into one of locating exchangeable cations.

This task has proven difficult even in fully dehydrated zeolites since there are invariably fewer cations than available sites. Furthermore, the distribution of mobile cations over several crystallographically distinct types of sites varies from sample to sample since the cation distribution is dependent on the negative charge distribution of the alumino-silicate framework, the cation size and charge, directional bond and coordination preference of the cation, and the solvation state of the zeolite.

In previous work on polyelectrolytic salts of copolymers, such as those of polyethylene-methacrylic acid, ionic oxide glasses (7), and various cation exchanged forms of β-alumina (8), we have observed mass-and site-dependent cation-site vibrations in the far infrared spectra. On the basis of this, we may expect such ion motion bands in the far infrared spectra of zeolites, and for them to be sensitive to solvation and other interactions involving the cations. Indeed, several interionic vibrations have been observed in monovalent exchanged zeolites X and Y (9) and the effect of hydration on the band structure studied (10). In this work we examine cation interactions

with several organic adsorbates to determine whether these molecules affect cation migration and examine the monovalent cation exchanged zeolites to assign the cation motion bands in greater detail. The spectra of divalent ion exchanged zeolites are also reported in conjunction with the relation between ionic vibrations and ionic conductivity.

The framework topology of zeolites X and Y, isotypical with the mineral faujasite, has been well characterized (11) and is distinguished by the largest known cavities and channels of all zeolites. With unit cell composition $M_x(AlO_2)_x(SiO_2)_{192-x}$ (x = 48-90), the alumino-silicate framework is a cross-linked crystalline macromolecule where each aluminum and silicon atom is tetrahedrally bonded to four bridging oxygen atoms. Twenty-four of these tetrahedrally bonded atoms make up each of the cubooctahedra (sodalite cages) which are in turn stacked in a tetrahedral diamond array so that adjacent Al,Si six-rings of the sodalite cages are joined via six shared oxygen atoms forming a hexagonal prism. The cavities enclosed by the lattice of sodalite cages are called supercages which also interconnect in a tetrahedral manner through channels consisting of 12-rings of Al,Si tetrahedra.

The designation of favorable cation sites and framework oxygens follows that of Smith (12). Cations on site I are centered in the hexagonal prisms and are coordinated octahedrally to six O_3 oxygens. The sixteen sites of this type per unit cell are inaccessible to species larger than 2.8 Å diameter such as H_2O and Cs^+. Sites I', II, and II' all provide one-sided three-fold coordination to oxygens of the sodalite cage six-rings. I' is within the sodalite cage but shares three O_3's of the bridging hexagonal prisms so that simultaneous cation occupancy of I and I' is unlikely. Sites II and II', within the supercage and the sodalite cage, respectively, are also mutually exclusive to cation occupancy since both share the same three O_2 oxygens of the free six-rings of the sodalite cages.

There are 32 of each of the asymmetric bonding sites per unit cell so that, depending on the occupancy of site I, 48-64 cations can be accommodated. This number is sufficient for the Y zeolites but not for X type zeolites. To account for these additional cations, various sites, collectively referred to as site III, have been proposed on the walls of the supercage. Mortier et al. (13) proposed a site affording one-sided square-planar coordination to two O_4 oxygens of the sodalite cage and two O_1 oxygens which bridge the cubooctahedra through hexagonal prisms. These squares come in pairs which share an edge of O_4's, therefore, only 48 of the 96 possible sites may be occupied due to steric as well as electrostatic reasons.

No monovalent cations have actually been located at such sites by X-ray structural studies not simply because of a low occupancy factor but probably because of large vibrational and static displacements of the ions. Highly unsymmetric bonding sites in hydrated and dehydrated CuY zeolites place some Cu^{2+} either on the edge of the square bonded unequally to O_1 and O_4 in natural faujasite (14) or in distorted three-fold coordination to an O_1, O_2, and O_4 which share the same T atom in synthetic faujasite (15). Even if monovalent ions larger than Cu^{2+}do not mimic its asymmetric bonding, the possibility of large anisotropic vibrations smearing the electron density remains. An intense high frequency dielectric relaxation in X zeolites has been attributed to cation motion over neighboring sites III with an activation energy in NaX of only 30 kJ mol^{-1} (16). This value is considerably lower than the activation energy for ionic conduction which involves a jump from site II to site III.

Upon hydration, a redistribution of cations is observed (12,13) in which the population of sites I, I', and II decrease and the number of unlocated cations in the supercage increases. A similar migration occurs in the presence of other adsorbents (17), but different cations have specific preferences for extraction by either small polar molecules or larger π-bonding ligands. Adsorbents can effect migration by delocalizing the framework charge, thus weakening the cation-framework attraction, and by directly bonding to or solvating the cations. Both direct and indirect cation-adsorbent interactions have been inferred through changes in the stretching frequency of adsorbed carbon monoxide (18) and changes in the epr line shape of Mn^{2+} doped zeolites (19). In this work, we have been able to associate far-infrared bands with cations on specific sites and through a study of the effects of adsorbents on these bands have been able to distinguish between direct and indirect cation-adsorbent interactions.

Experimental Section

The zeolites used in this study were supplied in exchanged form by the Linde Division of Union Carbide Corporation and were analyzed as presented in Table I. The balance of cations in each case is predominantly sodium although hydrolysis has been shown to occur to some extent under all aqueous exchange conditions (20).

Two far infrared sampling techniques were used with equal success. In one a petroleum jelly mull was held between low density polyethylene plates, and in the other the zeolite powder was supported on a transparent substrate in a vacuum ir cell. In both cases all zeolite powder samples were dehydrated by evacuating them under 10^{-4} torr vacuum for six hours and then slowly heating to 400°C (500°C for divalent zeolites) for 12 hours or until the pressure was less than 10^{-4} torr. With the mull process, the hot flask containing the zeolite was separated from the line, allowed to cool, then opened in a glove bag filled with dry nitrogen and immediately mulled with some previously dried petroleum jelly. When pressed between two polyethylene windows, such mulls may be exposed to air at little risk of becoming hydrated.

A silicon wafer mounted in a steel ring served as a substrate to an aqueous slurry of zeolite. After drying, the zeolite powder adhered reasonably well to the wafer during magnetic manipulation of the steel ring between the furnace portion of the vacuum cell and the spectral window portion. Since some sample was inevitably lost between runs, conclusions based on adsorbance changes are not quantitative.

The absorbates, tetrahydrofuran (THF), dimethylsulfoxide (DMSO), pyridine (pyr), CH_2Cl_2 and D_2O, were reagent grade and, except for the last, were freshly distilled over sodium or calcium hydride then vacuum degassed before use.

Dehydrated zeolites were cooled to room temperature before exposure to the solvents. The amount adsorbed was controlled by varying the temperature of the solvent, thus its vapor pressure, as well as the time of exposure, but gas analyses were not performed since it was our goal to simply induce spectral changes. For substrate mounted samples, the zeolites were exposed to 0.05 torr of the adsorbate for five minutes then reevacuated at room temperature for five minutes.

Infrared spectra were recorded on a Digilab FTS-14 interferometer at a resolution of 4 cm^{-1}. A smoothing function was used occasionally to reduce noise but resolution was never degraded below 8 cm^{-1}. Mull samples were referenced against air while a spectrum of the substrate sample cell with the silicon wafer out of the beam was stored as a reference for these samples.

Results

A. Monovalent Cation Containing Dehydrated Zeolites

The far infrared spectra of LiY and AgY shown in Figures 1 and 2 are reported for the first time and the spectra of the remaining alkali metal zeolites summarized in Tables II and III are similar to those reported by Brodskii et al. (9). Minor differences in band shapes and positions are expected due to differing synthetic histories of the samples which result in variations in Si, Al ordering and in the Si/Al ratio. The higher resolution of our spectra, however, has permitted the identification of a number of bands not observed by Brodskii.

Various bands have been assigned as interionic vibrations of cations on specific sites by considering the occupancy factors of the sites, the potential energy differences between sites, and the behavior of the bands in the presence of adsorbed gases. Site II is the most highly populated in dry monovalent cation Y zeolites and should give rise to the most intense band. A similar band at slightly higher frequency is expected in the corresponding X zeolites due to their more highly charged framework. There is little chance of site II cations in X being obscured by the more numerous site III cations since the latter are so weakly bonded that the frequencies at the two sites will be far from coincidence.

Site II' is vacant in these samples so there is no problem of accidental degeneracy from this source, but potential energy calculations by Dempsey (21) and Mortier (22) indicate that site I', which has a population comparable to site II, lies at only slightly higher energy. Since the strength of the three-

fold bonding to a 6-ring at I' is nearly indistinguishable from that at site II, the two vibrational bands will overlap considerably. The highest intensity low frequency band in these zeolites is therefore assigned in Tables II and III as representing cations on sites I' and II.

Potential energy calculations (21, 22) also indicate that site I is at a higher energy than site II in these samples. This does not necessarily mean that cation vibrations at this site will occur at a lower frequency than at site II since the octahedral coordination at site I may place a steric strain on the ion so that the vibrational frequency is higher. The fact that repulsions are dominant in raising the energy of site I is evident in zeolites exchanged with rubidium or cesium which are excluded from the hexagonal prisms. Since x-ray results indicate that the cation-oxygen distance at site I is greater than at site II in dry sodium and potassium zeolites, we conclude that steric repulsions are unimportant for these two ions and that the site I frequency should lie lower than the site II frequency. Furthermore, since the hexagonal prisms in sodium and potassium zeolites never contain more than ten cations per unit cell (13, 23), the site I vibrational bands will be relatively low intensity as reported in Tables II and III.

AgY is anomalous in that its site I is more stable than site II. Due to its high polarizability (2.4 $\mathring{A}^3$), the large silver ion is stabilized in the prisms through the formation of covalent bonds. In silver beta-alumina (24), the mobile ions occupy what would normally be considered a high energy site. Likewise in AgX and AgY, silver fills the hexagonal prisms in preference to other sites (12, 25). Nevertheless, the band arising from silver in the prisms

From the cation distribution, bands assigned to site III cations in X zeolites should not appear in Y zeolites. In the CsY sample, however, there are 37 cesium ions per unit cell which are more than can be accommodated on site II. The band at 30 cm^{-1} is accordingly assigned to the five or more Cs^{+} ions per unit cell occupying site III. This means that even at the temperature of dehydration of these samples cesium is excluded from the sodalite cage in contrast to the x-ray results for CsA zeolite (26) which found cesium in the small cavities. Apparently the higher silica content of Y reduces the six-ring opening sufficiently to maintain the exclusion of large ions. Considering the reduced framework charge of CsY relative to CsX, the frequency of the assigned band is reasonable and lends further support to this first indication of site III occupancy in a Y zeolite.

B. Divalent Cation Containing Dehydrated Zeolites

Because of their high charge/radius ratio, the ionic vibrations of divalent cations on the zeolite framework are expected to occur at significantly higher frequency than monovalent cations of similar mass. The spectra of alkaline earth exchanged Y and Ca exchanged X zeolites summarized in Table IV and illustrated in Figures 3 and 4 with CaY and BaY confirm this expectation.

From either Madelung potential calculations (21) or a consideration of cation site occupancy factors(12), site I is clearly the most stable in the dry zeolites, and cations at this location will have the highest vibrational frequency. In Y zeolites, the total population at the 16 sites I is nearly equal to that on all other sites combined, while in X zeolites, cations at I account for only one fourth of the total.

The ion motion band assignments for CaY and BaY fit the above prescription: a pair of bands of near equal intensity separated by 30 cm^{-1} with the higher frequency band assigned to ions on site I. In divalent cation zeolites, the band assigned to site II encompasses not only ions on I' as in monovalent cation zeolites but also II' which is found to be occupied in polyvalent cation zeolites due to the presence of tightly bound residual water in the sodalite cage. The pair of bands in CaX is more closely spaced than in CaY, but the lower energy absorption is more intense as expected. The two band pattern is not evident in SrY which has a single strong, broad absorption centered at 189 cm^{-1}. Ions at all sites are probably under this band envelope, so the assignment of site II strontium as the weak 150 cm^{-1} band on the side of this major peak is tenuous.

Unique among these zeolites is MgY since we have been unable to identify its cation motion bands. It is known that the small size and high field of Mg^{2+} enable it to substitute for aluminum in spinel-like structures, and although such replacement is unlikely at the dehydration temperature of 500 °C, the Mg-O vibrational modes will be strongly coupled with those of the framework. The interionic vibrations of Mg^{2+}, therefore, will be evident only in the shifted frequencies of framework modes.

C. Interactions with Adsorbed Molecules.

Upon adsorption of polar solvents, zeolites are able to approach their equilibrium state in which the framework charge is delocalized by the adsorbent. This charge delocalization will reduce the force constants and vibrational frequencies of non-sterically constrained cations. These exposed cations may also be partially solvated resulting in a further reduction of the vibrational

frequency. Both processes, solvation and charge delocalization, operate concurrently so that a steady decrease in the frequency assigned to site II cations is observed upon increasing the degree of hydration. This is illustrated in Figure 5 and 6 with KX and KY in which the site II vibrations shift from 156 cm^{-1} to 122 cm^{-1} and from 133 cm^{-1} to 114 cm^{-1}, respectively.

The site III vibration observed in X zeolites shifts negligibly in frequency at low degrees of hydration, but its apparent intensity declines dramatically. It is no longer observable in KX zeolites more than 50% hydrated. The disappearance of this band is matched by the growth of a new band at 177 cm^{-1} which had been attributed (10) to liquid water. We believe, however, that this high frequency band is due to ion motion of hydrated potassium ions and is analogous to ion motion bands observed in THF, DMSO, and pyridine solutions of the alkali metal salts of $Co(CO)_4^-$ and $Mn(CO)_5^-$ (27). Nearly as large a fraction of the ions in hydrated KY zeolite as in hydrated KX zeolite are unlocated by x-ray diffraction (13) and may be presumed to be "in solution" in the supercage. A similar high frequency band is therefore observed in KY at 149 cm^{-1} due to hydrated potassium.

There is no apparent change in the site I frequency in KY despite the increasing charge delocalization with hydration level. This is probably due to a relaxation of strong lattice distortions that result in a $K(I)-O_3$ distance that is shorter in hydrated than dehydrated samples (13). The spectra of Figure 6 provide no evidence for solvent extraction of ions from site I because of the increased overlap of this band with the shifting site II band.

D. Polar Organic Adsorbates

On the basis of complete volume filling of the large cavities, the limiting adsorption values for the large molecules studied here, pyridine, tetrahydrofuran, demethylsulfoxide, and dichloromethane, will be considerably less than the limiting value for water. The void volume of Y zeolites is nearly as great as in NaX which can hold a maximum of six of these large molecules per supercage compared to over 30 water molecules per supercage (28). This inherently low coverage by the organic compounds will affect the cation vibrations in two ways. First, delocalization of the framework charge will not be as effective as in hydrated zeolites resulting in a less pronounced low energy shift of the site II cation band. Second, direct cation-adsorbate interaction involving all supercage ions is possible only in Y zeolites. Two of the eight ions per supercage in dry NaX and KX will be affected only indirectly and the number of unaffected ions will be even greater if some ions achieve a solvent coordination number greater than one.

As can be seen from the absorbance spectra of Figures 7 - 9 in which zeolites NaX and KX have been exposed to 0.05 torr of the various adsorbents, the expected shift of the site II band to lower frequencies is less pronounced with sodium than with potassium. The 190 cm^{-1} band of dehydrated NaX shifts to only 180 cm^{-1} even in fully solvated or hydrated samples. On the other hand, corresponding levels of solvation in KX samples produce a shift in the site II potassium band more than twice as great as in NaX samples. This contrasting behavior reflects the extent of cation exposure to the supercage. Sodium ion, due to its smaller size, resides almost in the plane of the six-ring and is thereby screened to a large extent from direct interaction with

adsorbed molecules in the supercage while the larger potassium ions are held well above the plane in trigonal pyramidal coordination to the O_2 oxygens. The shielding nature of planar or near-planar coordination is in agreement with a vibrational analysis of alkali metal ions encaged in a planar cyclic polyether (29) in which the cation motion frequencies are unperturbed by the presence of various organic molecules or anions. An alternative explanation of the more pronounced shift of potassium versus sodium ion frequencies in X zeolites is that the solvent interacts only indirectly with site II ions and that delocalization of the framework charge has the least effect on cations held in near-planar coordination. This model of solvent behavior is supported by the results for solvated KY zeolites discussed at the end of this section.

The most symmetric geometry of the solvated ion, ML_n^+, when n = 2, 3, or 4 will be linear, trigonal planar, and tetrahedral, respectively. Assuming that the local symmetry about the cation, $D_{\infty h}$, D_{3h}, or T_d, dominates the spectral selection rules, only the asymmetric stretching mode will be infrared active while the symmetric stretching mode is Raman active only. However, if these three structures are distorted, the symmetry is lowered and both the symmetric and asymmetric vibrations become infrared active. In the NaX spectra of Figures 7 and 8, a new band appears at higher and lower frequency than the site II band. The lower frequency band which grows in near 155 cm^{-1} is coincident with the weak shoulder already assigned to site I sodium, and the higher frequency band near 215 cm^{-1} is almost coincident with a weak framework mode at 220 cm^{-1}. Together, these two bands are assigned as the symmetric and antisymmetric vibrations, respectively, of cations with distorted solvent coordination.

The presence of a solvated ion motion band at higher frequency than the site II mode is consonant with the results for hydrated zeolites, but the assignment of the lower frequency band as another mode of the same species requires further explanation. It would be tempting, for example, to assign this band to sodium ions migrating into site I, but this is contrary to the observation that migration, if it does occur, is out of site I (17). Another alternative would be to assign the 155 cm^{-1} band to a sodium vibration on site II weakened by direct interaction with the adsorbate. This would mean that the main site II band is shifted only slightly from 190 cm^{-1} due to charge delocalization effects alone. Although attractive, this last explanation is not tenable because the low frequency band disappears in moderately hydrated samples. The 155 cm^{-1} band grows in at low hydration levels as with the organic solvents but then completely disappears at moderate to full hydration leaving only the site II band at 180 cm^{-1} and the solvated ion band at 215 cm^{-1}. This indicates that at low hydration levels and at all solvation levels with the organic adsorbates, the limited amount of solvent bonds unsymmetrically to cations considered in solution in the supercage. Of the solvents studied, only water molecules can occupy the supercages in sufficient number to provide a high symmetry field around each cation which causes the symmetric stretching vibration to disappear.

The two modes of the same solvated species appear in the KX spectra as shoulders on the site II band at 120 cm^{-1} and 165 cm^{-1}. As in the NaX samples, the growth of these bands is accompanied by a decrease in the intensity of the site III band. The symmetric and antisymmetric modes also appear in the spectra of KY zeolite at 115 cm^{-1} and 155 cm^{-1} as shown in Figure 10. In fully solvated samples, these two shoulders become almost as intense as the site II band.

At low solvation levels, the site II band of KY at 133 cm^{-1} shifts two to three wavenumbers higher in frequency and at full solvation moves only three to four wavenumbers lower in frequency. A direct adsorbent-site II cation interaction should result in a more dramatic low energy shift, so this result indicates that the adsorbates preferentially solvate ions in the supercage. There are 20 cations per unit cell unlocated by x-ray of hydrated KY and 20 cations on site II, and if a similar distribution obtains in solvated zeolites, the maximum of 48 large molecules per unit cell will leave the free supercage ions well below the optimum coordination of four ligands. With all the adsorbates molecules thus involved in solvating free supercage cations, the site II vibrational frequency will be affected only indirectly by charge delocalization, and since there is less charge to be delocalized in Y than in X, the frequency shift is less.

DISCUSSION

Among the dehydrated zeolites, several bands are observed in each case and attributed to cations on different crystallographic sites. Our confidence in the band assignments is buttressed by the fact that there is a nearly linear relation between the frequencies of site II or site III vibrations in each zeolite and $m^{-1/2}$ for each cation. The deviation from linearity shows an interesting relation between the cation-framework force constant and the cation size and framework charge: in Y zeolites, the force constant decreases slightly with increasing cation size, but in X zeolites, the force constant increases slightly with cation size indication that secondary electrostatic interactions become significant in the more highly charged zeolite. The force constants, calculated assuming a symmetric vibration and a rigid framework with the expression $k = 4\pi^2\nu^2\mu$ and $\mu \simeq M$, are listed in Table V. The anomalously high value for LiY is probably due to the fact that lithium ion is 6-coordinate at site II rather that 3-coordinate.

The site II cation-framework force constants in Y zeolites should be related to the activation energy of ionic conduction if the rate determining step is a jump from site II to site III. This relation is evident in the Rice and Roth model of ionic transport in super-ionic conductors (30), which presumes that the conducting ions may be thermally excited from their ionic sites above an energy gap, ε_o, so that they propagate through the lattice with a velocity, v_m, and a mean free path, l_m, to another localized ionic site. By relating (31), their expression for ionic conductivity to that of conventional hopping models, the energy gap, ε_o, is equal to the activation energy required to effect an ionic hop and

$$E = \frac{1}{2} M v_o^2 a_o^2$$

where M is the cation mass, ν_o is the vibrational frequency of the ion at a localized site, and a_o is the hopping distance between a cation and a vacant neighboring site. The dependence of the activation energy on the rigid lattice force constant and the hopping distance was recently applied to inorganic oxide glasses (31).

The most probable hopping distance in Y zeolites, site II - site III, varies with the size of the cation in the same way as the force constant and tends to lower the activation energy. The calculated energies listed in Table VI are in reasonable agreement with experimental values and require far fewer approximations than electrostatic calculations.

The observed activation energies of LiX and NaX are lower than those of the corresponding Y zeolite but the energies of K, Rb, and CsX are the same as in Y (16) due to cation-cation repulsions between sites II and III. (Such repulsions also account for the large observed E_a in CsY.) The rate determining step does not appear to be the same in X zeolites as the simple II → III jump in Y zeolites because the higher force constants in X will make E_a systematically too high. Likewise, a jump for III → II involving the site III force constants results in activation energies systematically too low and leads to a dead end since site III must ultimately be repopulated. Although there are other possible single jump mechanisms to calculate, they are all suspect, since all of the supercage ions contribute to the conductivity and only one activation energy has been observed. A more likely approach is the intersticialcy pair mechanism invoked by Wang et al. (32) to explain transport in β-alumina in which the movement of one ion displaces another. Since the Rice and Roth free-ion model is only approximate

at best and is only suited for cases in which there are readily available sites, it should not be expected to apply to a pair mechanism. It appears to apply usefully only when the motion of each ion may be considered to be an approximately independent event.

Another factor affecting the conductivity is the presence of residual sodium in Li, Rb, and Cs exchanged samples. The total number of supercage ions is greater in the last two cases than in the sodium zeolites resulting in the framework charge in the small cages being not as effectively enutralized. Accordingly, the site I Na frequency increases as noted in Tables II and III. In RbX and CsX, about 2/5 of the residual sodium is in the supercages and will have the effect of increasing the activation energy if cooperative interactions are predominant.

Most of the residual sodium in divalent exchanged samples is at site II. Exchange with divalent ions inevitabley leaves some of the negatively charged aluminum tetrahedra only indirectly compensated. As a consequence, the local framework charge experienced by the remaining Na will be greater and the site II Na vibrational frequency is seen in Table IV to increase relative to pure sodium zeolite. The smaller number of ions and the larger number of vacancies in divalent zeolites is well suited to the free ion model of ionic conduction but the only conductivity measurements on these zeolites pertain to hydrated samples (23) or organic solvents (33).

Acknowledgment

We are grateful for the valuable assistance of Mr. Carl Chalek in this work. This work was supported in part by the Office of Naval Research. We gratefully acknowledge that support and the support and use of facilities of the Materials Science Program of Brown University.

References

1a. P. A. Jacobs and J. B. Uytterhoeven, J. Catal., 26, 175 (1972).

b. P. A. Jacobs, B. K. G. Theng, and J. B. Uytterhoeven, J. Catal., 26, 191 (1972).

2. A. Bielanski and J. Datka, J. Catal., 32, 183 (1974).

3. P. E. Riley and K. Seff, J. Phys. Chem., 79, 1594 (1975).

4. P. Pichat, J. C. Vedrine, P. Gallezot, and B. Imelik, J. Catal., 32. 190 (1974).

5. D. J. C. Yates, J. Phys. Chem., 70, 3693 (1966).

6. G. T. Kerr, Advan. Chem. Ser., 121, 219 (1973).

7a. A. T. Tsatsas, J. W. Reed and W. M. Risen, Jr., J. Chem. Phys. 55, 3260 (1971)

b. G. J. Exarhos, P. J. Miller and W. M. Risen, Jr., J. Chem. Phys. 60, 4145 (1974).

8. W. M. Butler and W. M. Risen, Jr., submitted for publication.

9. I. A. Brodskii, S. P. Zhdanov, and A. E. Stanevich, Sov. Phys. Solid State, 15, 1771 (1974).

10. I. A. Brodskii, S. P. Zhdanov, and A. E. Stanevich, Opt. Spektrosk., 30, 58 (1971).

11. W. M. Meier and D. H. Olson, Advan. Chem. Ser., 101, 155 (1971).

12. J. V. Smith, Adv. Chem. Ser., 101, 171 (1971).

13a. W. J. Mortier and H. J. Bosmans, J. Phys. Chem., 75, 3327 (1971).

b. W. J. Mortier, H. J. Bosmans, and J. B. Uytterhoeven, J. Phys. Chem., 76, 650 (1972).

14. I. E. Maxwell and J. J. deBoer, J. Phys. Chem., 79,1874 (1975).

15. J. Marti, J. Soria, and F. H. CAno, J. Phys. Chem., 80, 1776 (1976).

16. F. J. Jansen and R. A. Schoonheydt, J. Chem. Soc., Faraday Trans. 1, 69, 1338 (1973).

17a. P. Gallezot, Y. Ben Taarit, and B. Imelik, J. Catal., 26, 295 (1972).

b. P. Gallezot, Y. Ben Taarit, and B. Imelik, J. Phys. Chem., 77, 2556 (1973).

18. C. L. Angell and P. C. Schaffer, J. Phys. Chem., 70, 1413 (1966)

19. N. N. Tikhomirova, I. V. Nikolaeva, E. N. Rosolovskaya, V. V. Demkin, and K. V. Topchieva, J. Catal., 40, 61 (1975)

20. A. Maes and A. Cremers, Advan. Chem. Ser., 121, 230 (1973)

21. E. Dempsey, J. Phys. Chem., 73, 3660 (1969)

22. W. J. Mortier, J. Phys. Chem., 79, 1447 (1975)

23. M. L. Costenoble cited by R. A. Schoonheydt, W. DeWilde, and F. Velghe, J. Phys. Chem., 80, 511 (1976)

24. W. L. Roth, J. Solid State Chem., 4, 60 (1972)

25. L. P. Aldridge and C. G. Pope, J. Inorg. Nucl. Chem., 36, 2097 (1974)

26. P. E. Riley and K. Seff, J. Phys. Chem., 79, 2163 (1975)

27. W. F. Edgell, J. Lyford, IV, R. Wright, W. Risen, Jr, and A. T. Watts, J. Amer. Chem. Soc., 92, 2240 (1970)

28. M. M. Dubinin and V. A. Astakhov, Advan. Chem. Ser., 102, 69 (1971)

29. A. T. Tsatsas, R. W. Stearns, and W. M. Risen, Jr., J. Amer. Chem. Soc., 94, 5247 (1972)

30. M. J. Rice and W. L. Roth, J. Solid State Chem., 4, 294 (1972)

31. G. J. Exarhos, P. J. Miller, and W. M. Risen, Jr., Solid State Commun., 17, 29 (1975)

32. J. C. Wang, M. Gaffari, and S. Choi, J. Chem. Phys., 63, 772 (1975)

33. A. Dyer and R. B. Gettins, J. Inorg. Nucl. Chem., 32, 2401 (1970)

34. J. W. Ward, Advan. Chem. Ser., 101, 380 (1971)

35. a. A. V. Kiselev, V. I. Lygin, and R. V. Starodubceva, J. Chem. Soc., Faraday Trans. I, 68, 1793 (1972)

    b. V. K. Chuikina, A. V. Kiselev, L. V. Mineyeva, and G. G. Muttik, J. Chem. Soc., Faraday Trans. I, 72, 1345 (1976)

Figure Captions

1. Far infrared transmittance of LiY zeolite
2. Far infrared transmittance of AgY zeolite
3. Far infrared transmittance of CaY zeolite
4. Far infrared transmittance of BaY zeolite
5. Far infrared transmittance of KX zeolite dry, hydrated, and approximately 50% hydrated
6. Far infrared transmittance KY zeolite at various degrees of hydration.
7. Absorbance spectra of dry NaX zeolite exposed to 0.05 torr H_2O, pyridine, and dimethyl sulfoxide.
8. Absorbance spectra of dry NaX zeolite exposed to 0.05 torr tetrahydrofuran and dichloromethane.
9. Far infrared absorbance of dry KX zeolite exposed to 0.05 torr of the indicated adsorbents.
10. Far infrared absorbance of dry KY zeolite exposed to 0.05 torr of the indicated reagents.

Table I

Composition of Zeolites

Zeolite	SiO_2/Al_2O_3	% Cation Analysis
LiY	4.83	47
NaY	4.95	92
KY	4.91	97
CsY	4.89	66
AgY		95
MgY		72
CaY		77
SrY		76
BaY		79
NaX	2.43	100
KX		73
CaX		75

Table II

Far Infrared Bands of Monovalent Cation Y Zeolites

assignment	LiY	int	NaY	int	KY	int	CsY	int	AgY	int
III	..		..		..		30	w sh	..	
I	..		167	m sh	107	m sh	..		50	w
II	380	sh	180	s	133	s	62	s	82	m
	100	w	122	m	..		109	m	122	w
	..		..		..		..		150	w
	164*	w	..		160	w sh	174*	m	168	vw
	212	w	..		..		210	w sh	228	w sh
	296	sh	273	m	270	w sh	280	w sh	270	w sh
	311	m	..		310	w sh	317	w sh	320	vw sh
ring def	396	s	392	s	385	s	383	s	380	s

* due to residual sodium

Table III

Far Infrared Bands of X Zeolites

assignment	NaX	int	KX	int	RbX	int	CsX	int
III	67	wm	58	m	48	wm	39	wm
I	160	w sh	..		..		..	
II	190	ms	156	s	108	ms	86	m
	91	w	77	vw	83	w sh	64*	w sh
	109	w	106	wm	118	w sh	126	m
	..		..		182*	m	188*	m
	..		..		204*	m	199*	m
	218	vw	230	w	..		..	
	263	w	277	vw sh	259	vw sh	254	w
	295	w	308	w sh	296	w	295	w
	321	w sh	322	m sh				
	..		357	w sh				
ring def.	382	s	373	s				

* due to residual Na

Table IV

Far Infrared Bands of Divalent Cation Zeolites

assignment	MgY	int	CaY	int	SrY	int	BaY	int	CaX	int
II	..		227	m	150	w	107	s	273	m
I	..		256	m	189	ms	137	s	287	wm
	..		40	w	53	w sh	50	w sh	50	w sh
	64	w sh	65	vw sh	67	w sh	60	w sh	65	w
	84	w	90	w sh	100	m	90	w sh	85	w
	..		..		..		..		100	w
	132	w	131	ms	122	w	..		132	w sh
	157	m	162	vw	165	w sh	157	wm	152	w
	..		170	vw	177	vw sh	182	w sh	168	wm
	190*	w	202*	w	204*	w sh	200*	w sh	200*	w sh
	..		211	vw	220	w	..		210	w
	249	w sh	..		250	wm	227	w sh	220	wm
	275	m	267	w sh	266	w	270	w sh	..	
	..		308	w sh	304	wm	310	m	321	m
	332	wm	..		330	wm	343	w	359	w sh
ring def.	401	s	385	m	385	s	375	s	380	s

* due to residual sodium

Table V

Cation - Rigid Framework Vibrational Force Constants (mdyn/Å)

zeolite	site II	zeolite	site II
LiY	0.59	CaX	1.76
NaY	0.44	CaY	1.22
AgY	0.43	SrY	1.16
KY	0.41	BaY	0.93
CsY	0.30		

zeolite	site II	site III
NaX	0.49	0.06
KX	0.56	0.08
RbX	0.59	0.12
CsX	0.58	0.12

Table VI

Activation Energy of Ionic Conductivity

zeolite	E_a^{expt} (ref 16) (kJ mole^{-1})	a_o (ref 16) (Å)	ν_o (cm^{-1})	E_a^{calc} (kJ mole^{-1})
LiY	90.3	5.02	380	113
NaY	74.2	4.62	180	71.6
KY	54.9	4.09	133	50.5
CsY	58.0	3.76	62	33
AgY	--	4.19	82	57

Table VII

Calculated Free Path for III → III Transition

zeolite	E_a (ref 16) (kJ mole^{-1})	ν_o (cm^{-1})	free path (calc) (Å)
NaX	52.3	67	10.6
KX	54.7	58	9.6
RbX	67.4	48	8.7
CsX	55.5	37	8.2

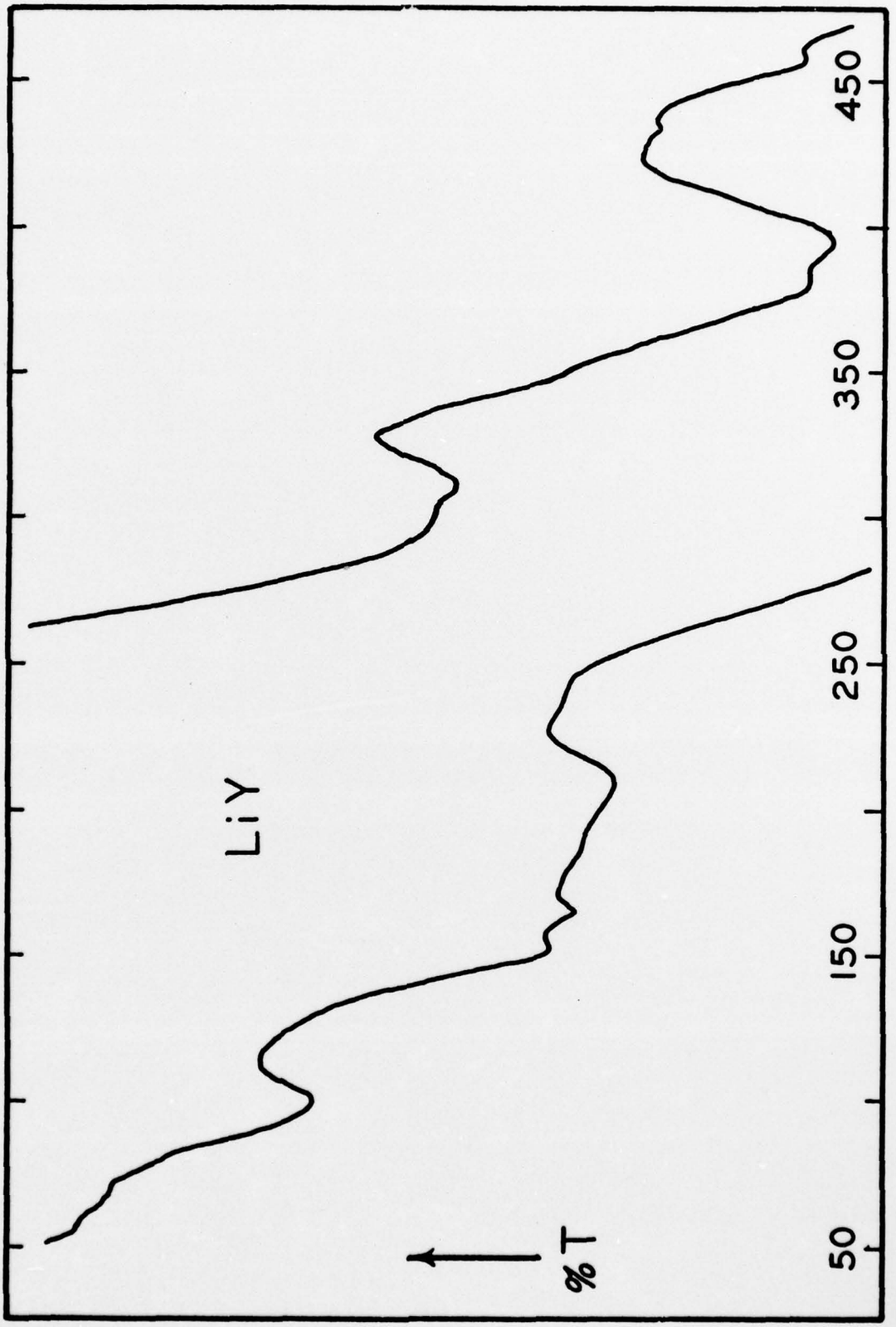
LiY
%T
50
150
250
350
450

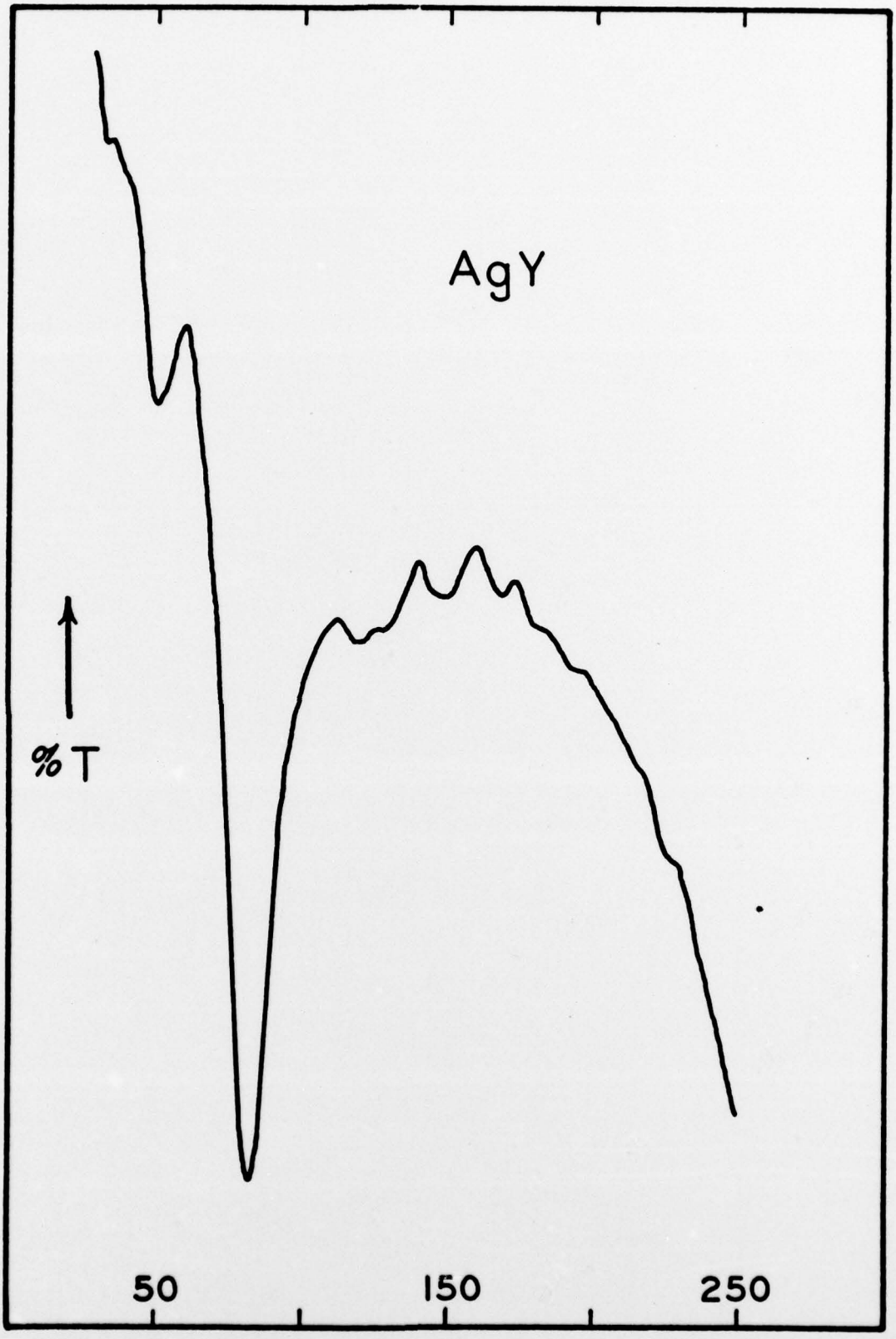
AgY
%T
50
150
250

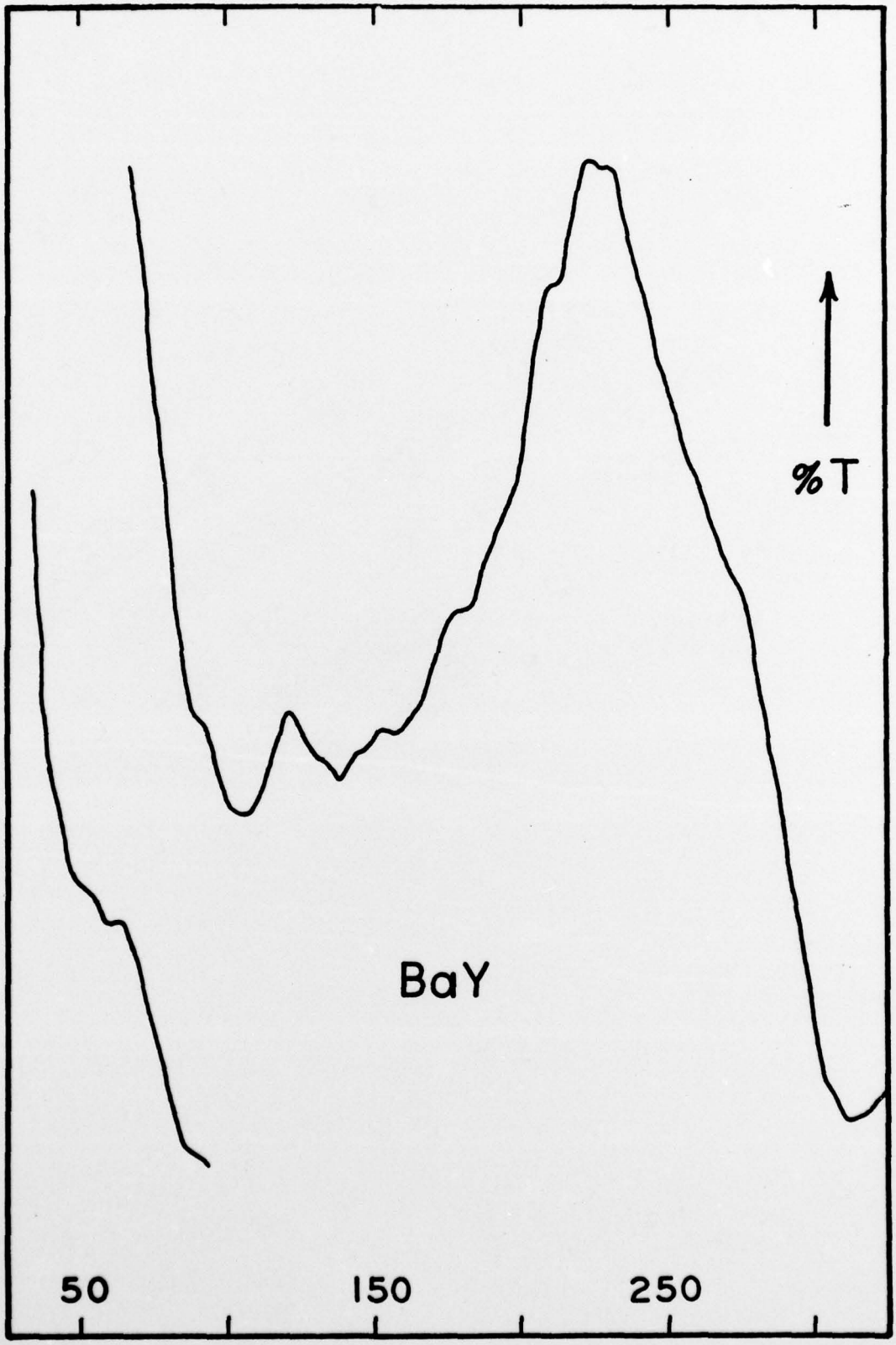
%T
BaY
50
150
250

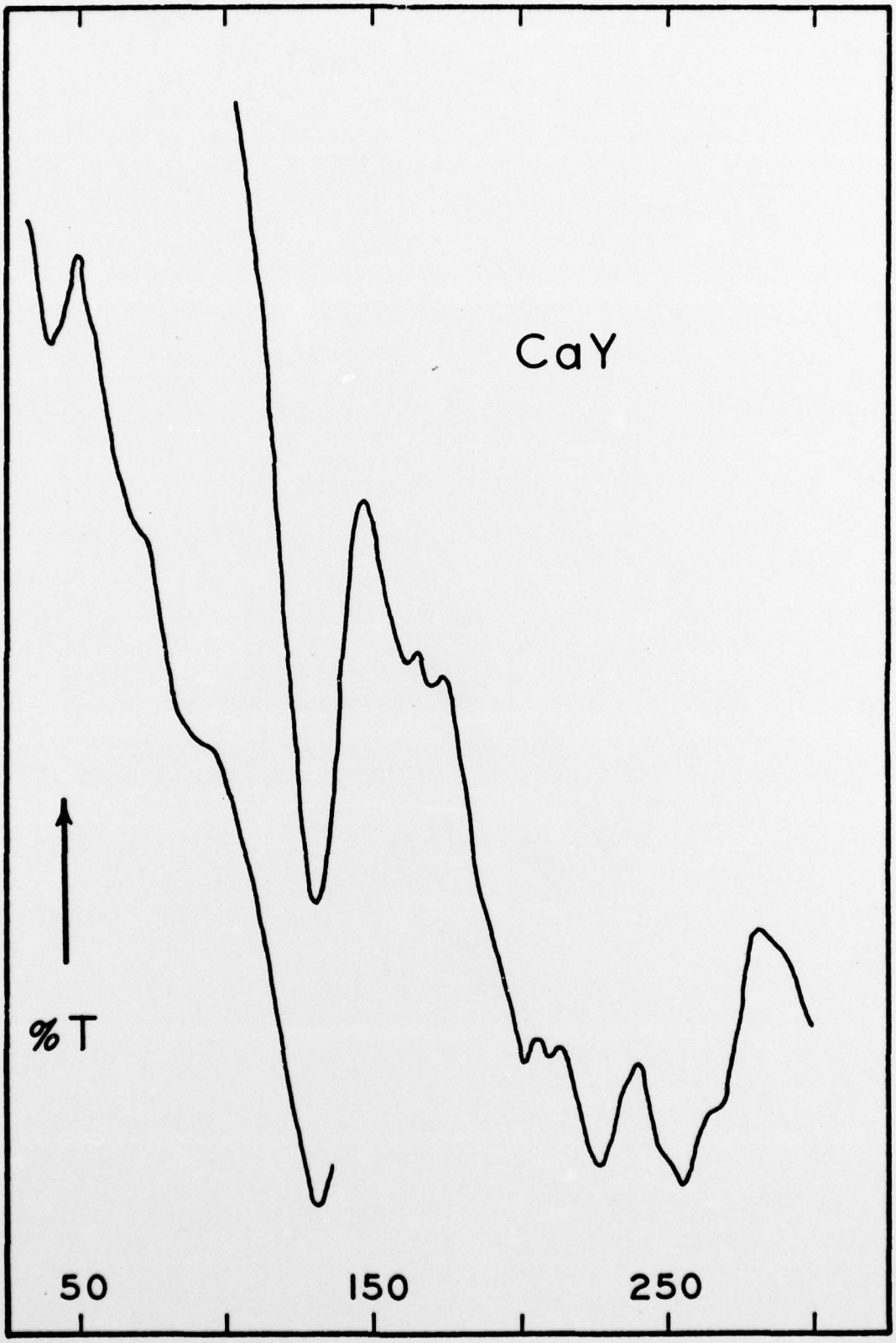
CaY
%T
50
150
250

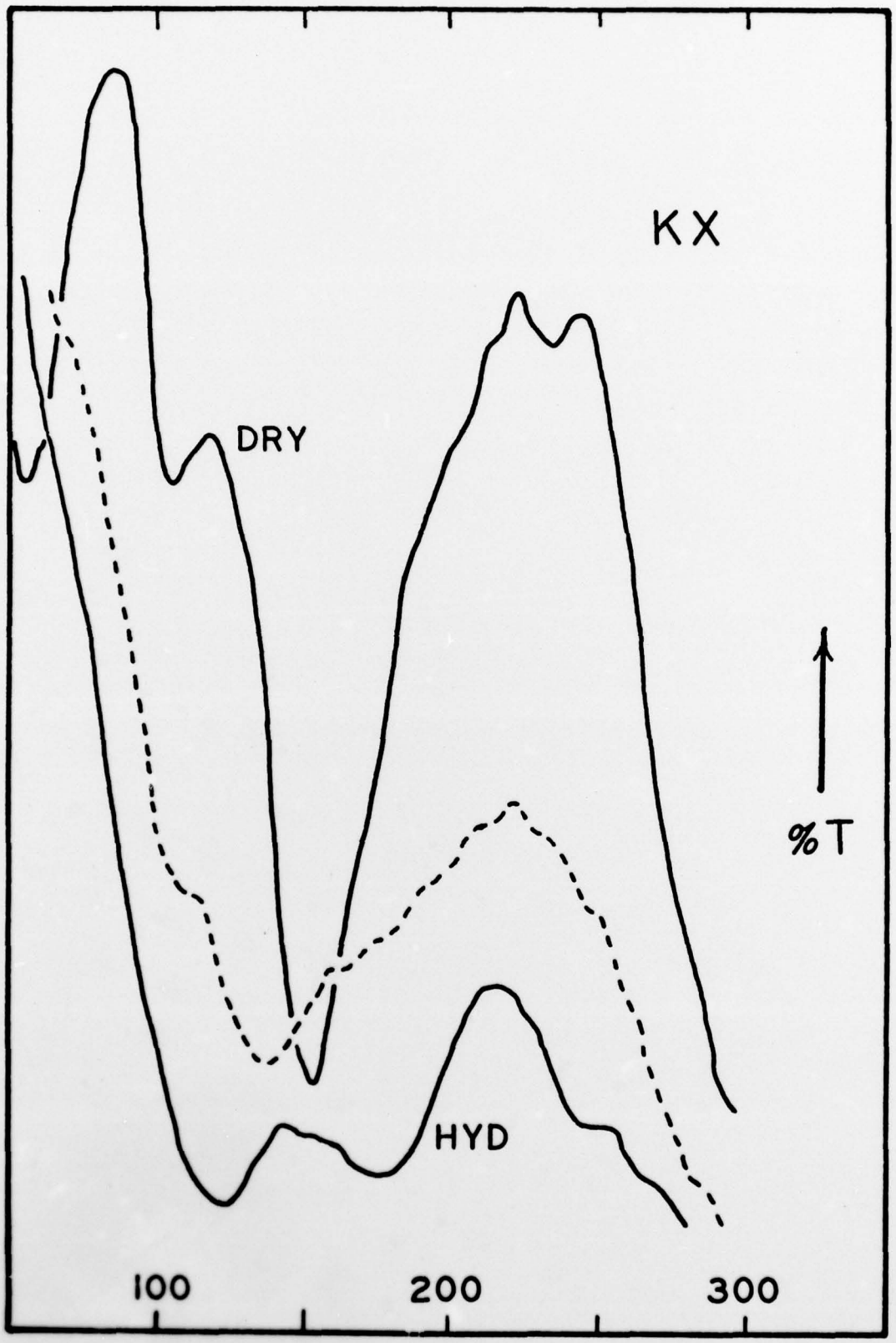
KX
DRY
HYD
%T
100
200
300

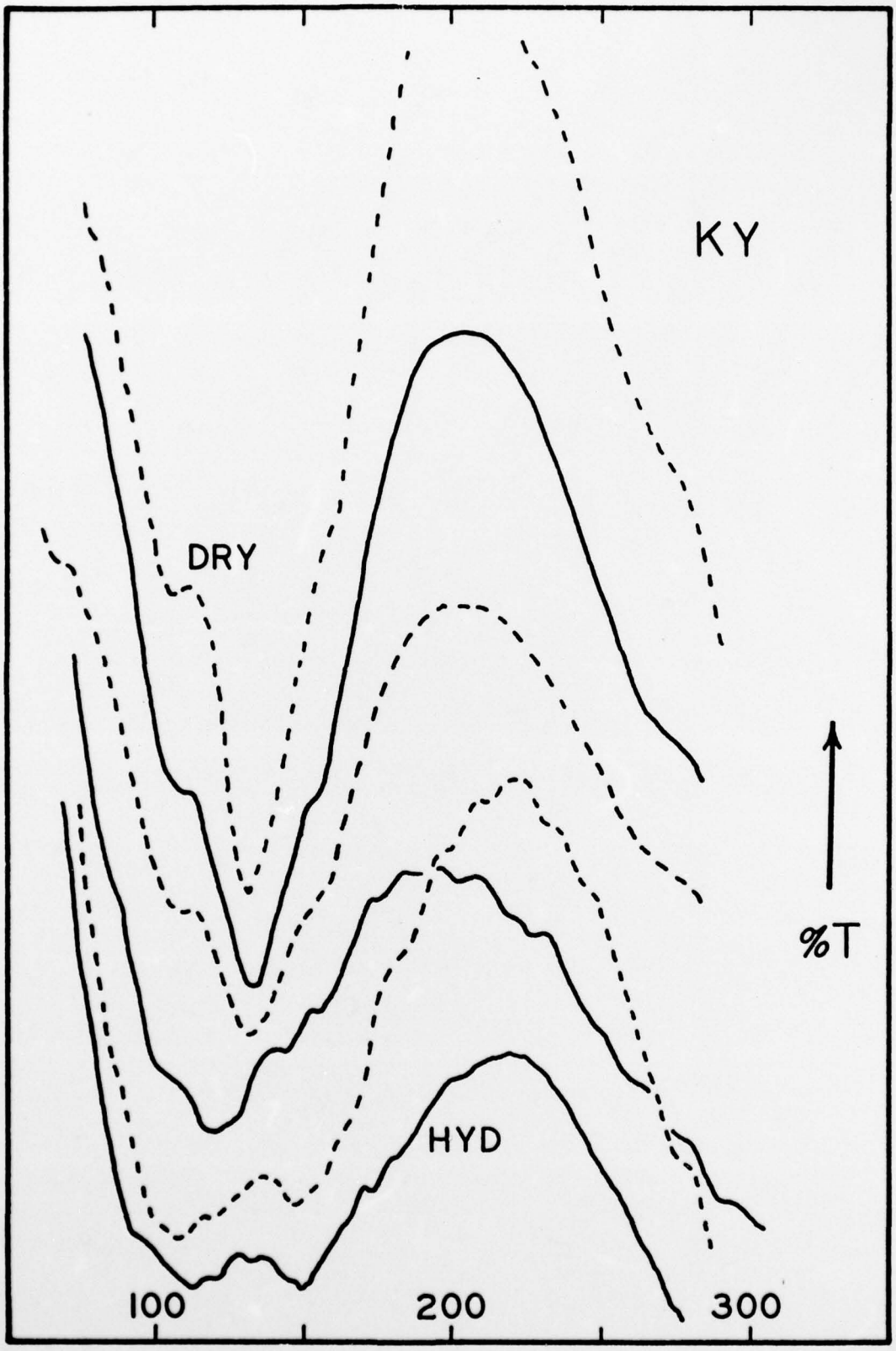
KY
DRY
HYD
%T
100
200
300

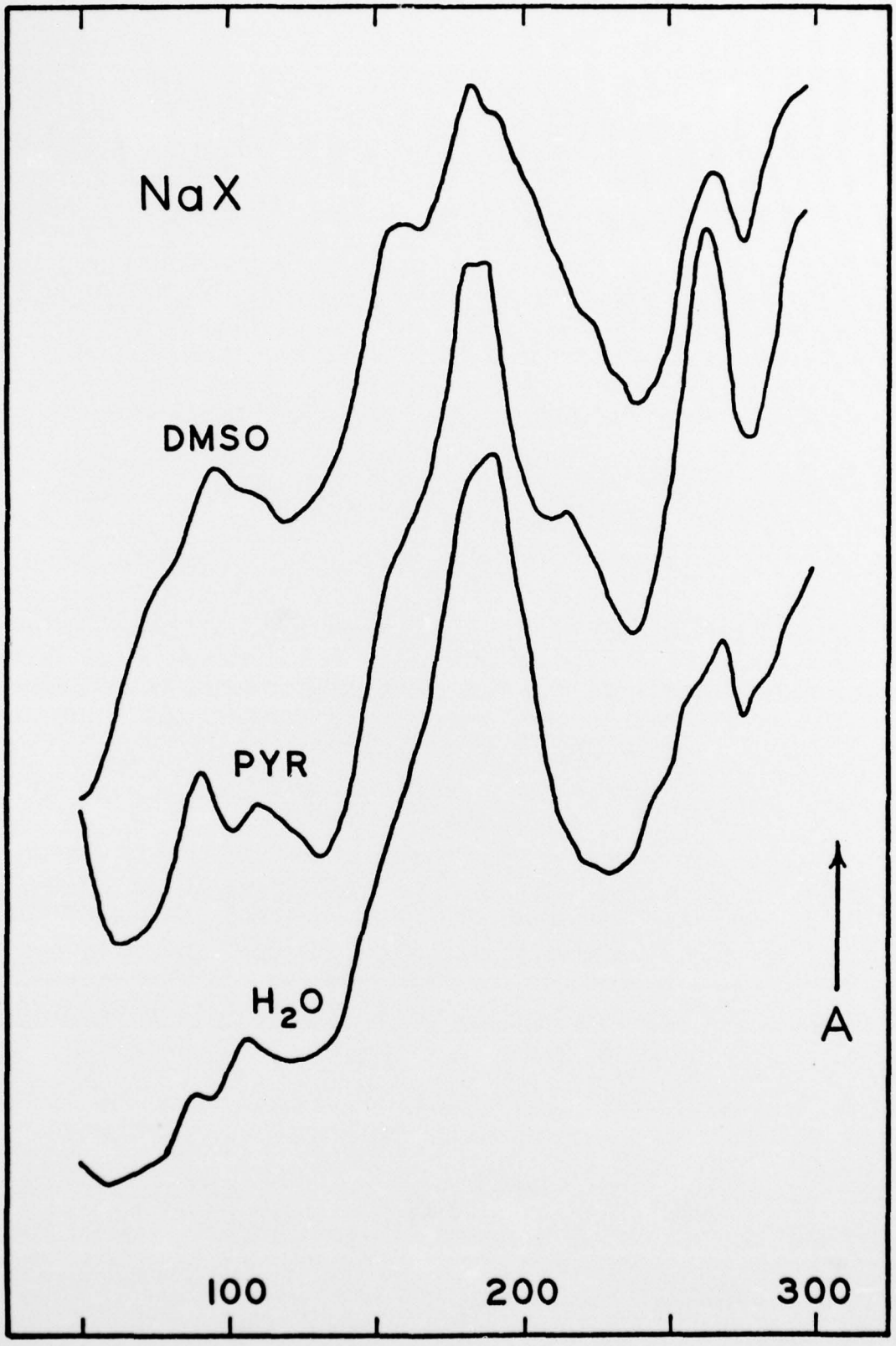
NaX
DMSO
PYR
H_2O
A
100
200
300

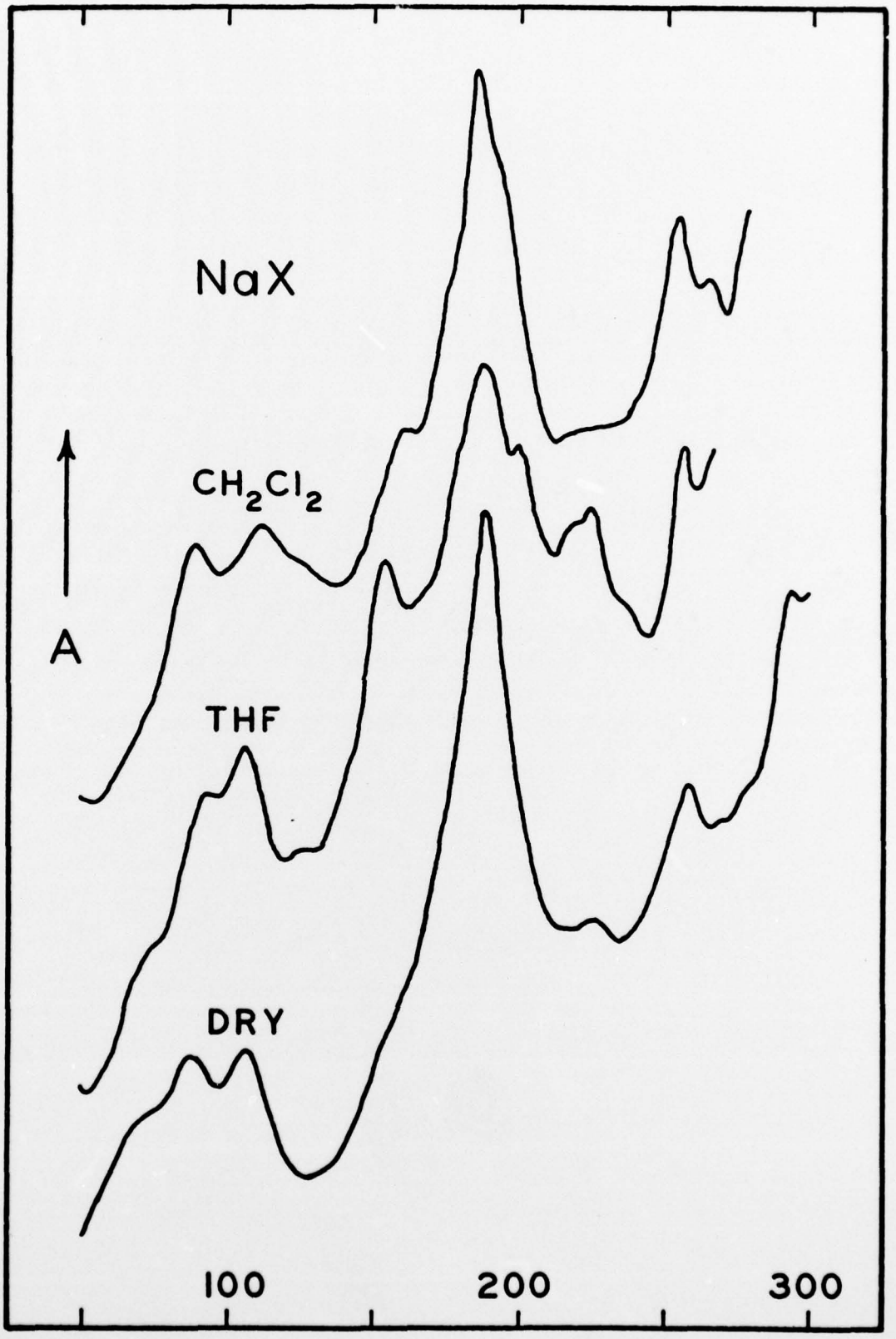
NaX
CH_2Cl_2
A
THF
DRY
100
200
300

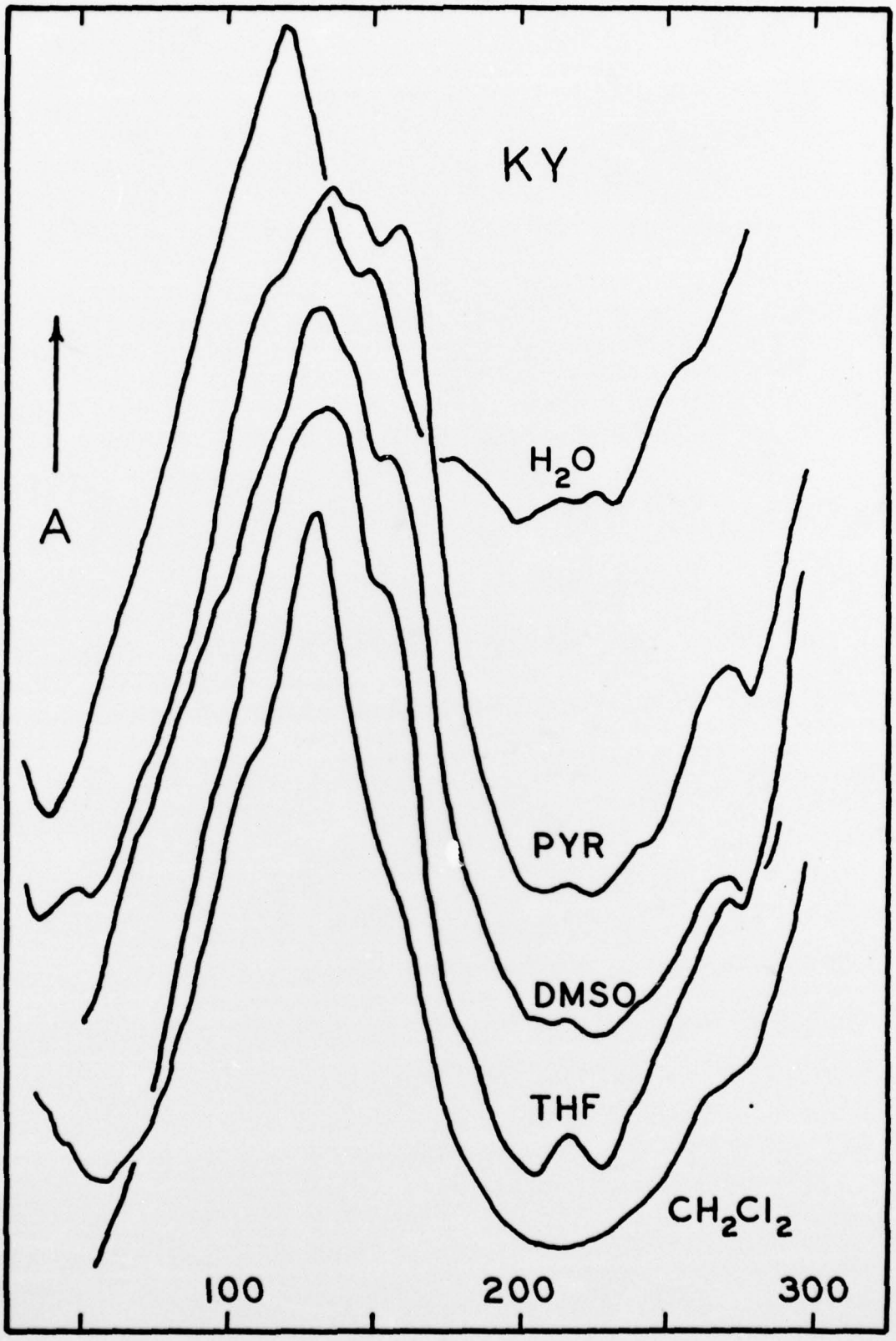
KY
A
H_2O
PYR
DMSO
THF
CH_2Cl_2
100
200
300

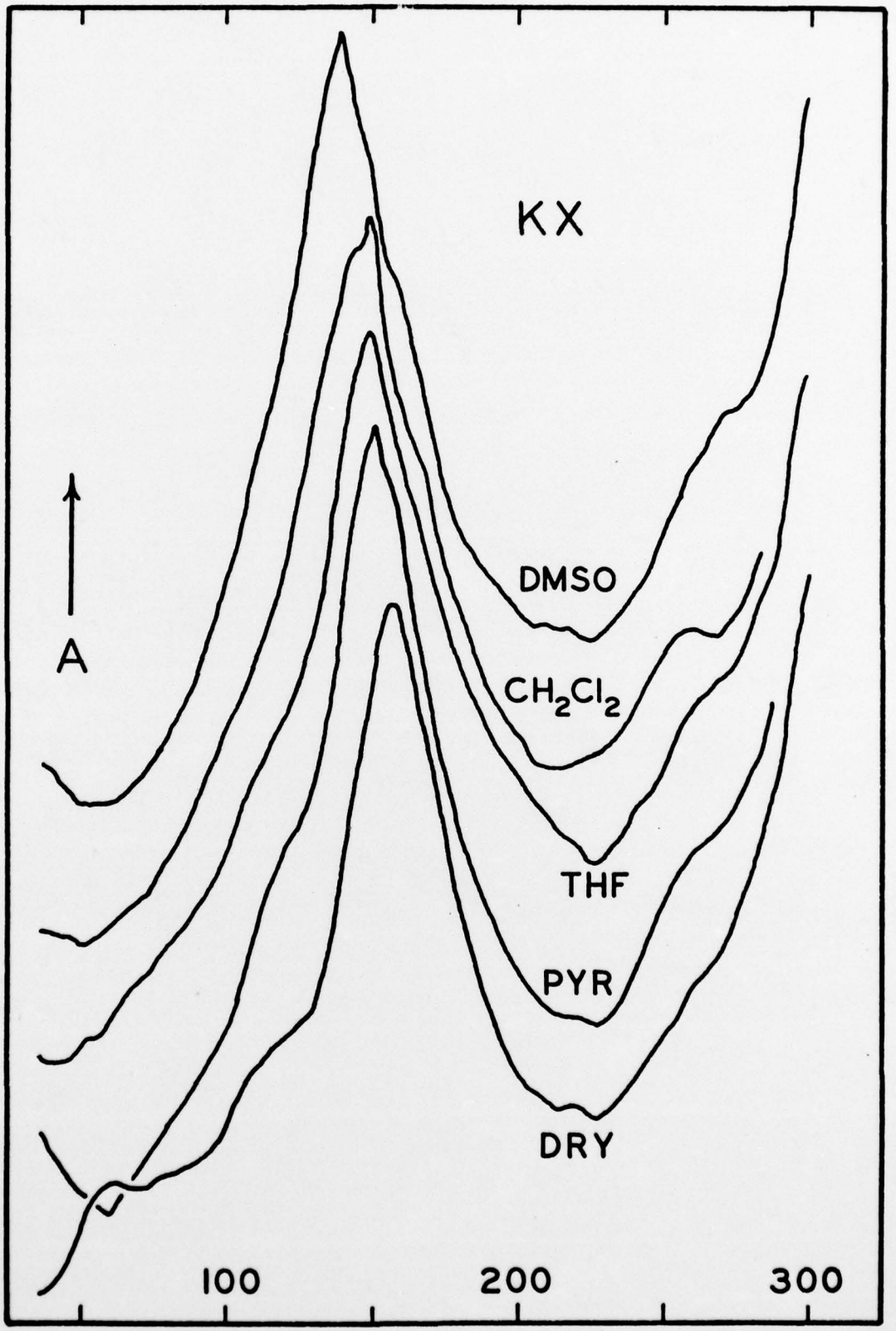
KX
A
DMSO
CH_2Cl_2
THF
PYR
DRY
100
200
300

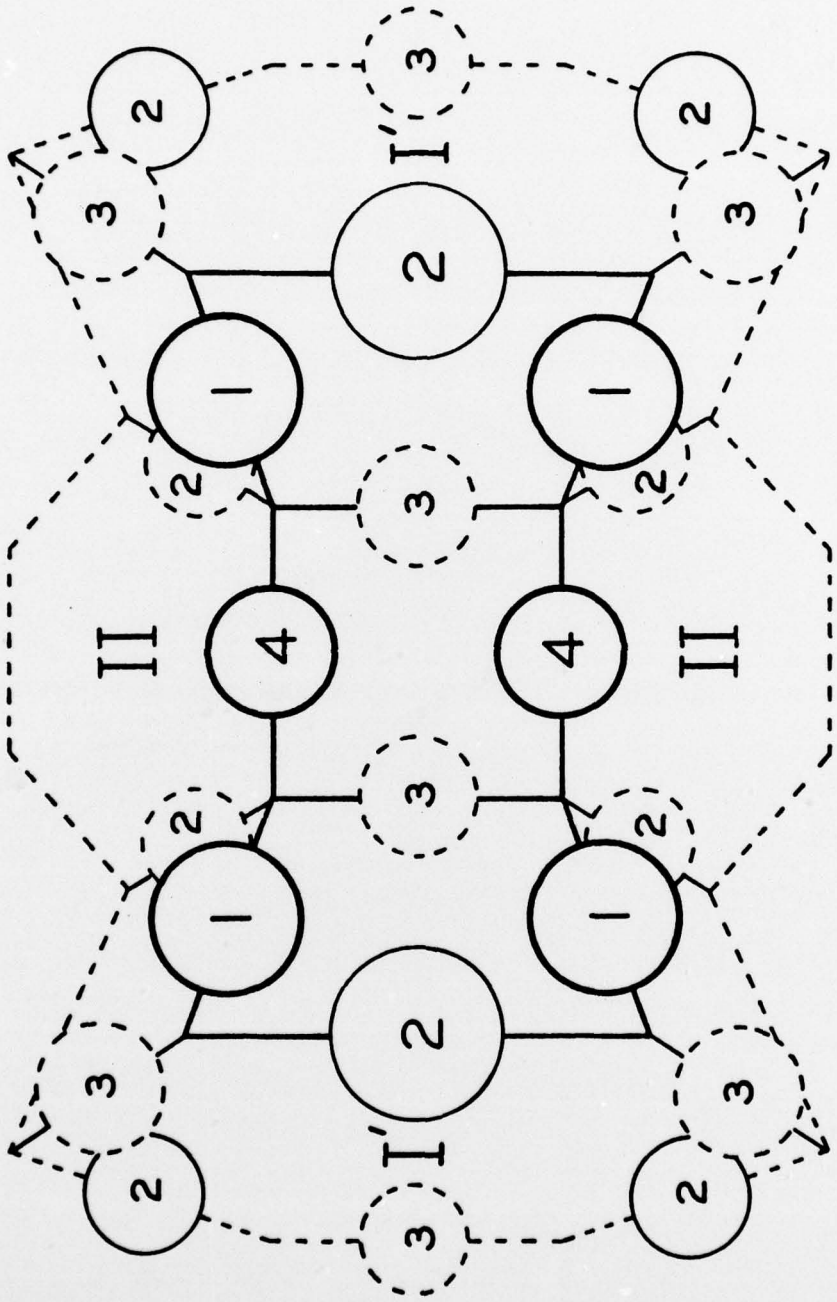
I
II
II
I
1
2
3
4

TECHNICAL REPORT DISTRIBUTION LIST

	No. Copies
Office of Naval Research Arlington, Virginia 22217 Attn: Code 472	2
Office of Naval Research Arlington, Virginia 22217 Attn: Code 1021P	6
ONR Branch Office 536 S. Clark Street Chicago, Illinois 60605 Attn: Dr. George Sandoz	1
ONR Branch Office 715 Broadway New York, New York 10003 Attn: Scientific Dept.	1
ONR Branch Office 1030 East Green Street Pasadena, California 91106 Attn: Dr. R. J. Marcus	1
ONR Branch Office 760 Market Street, Rm. 447 San Francisco, California 94102 Attn: Dr. P. A. Miller	1
ONR Branch Office 495 Summer Street Boston, Mass. 02210 Attn: Dr. L.H. Peebles	1
Director, Naval Research Lab. Washington, D. C. 20390 Attn: Library, Code 2029 (ONRL)	6
Technical Info. Div.	1
Code 6100, 6170	1
The Asst. Secretary of the Navy (&D) Dept of the Navy Room 4E736, Pentagon Washington, D. C. 20350	1
Commander, Naval Air Systems Command Department of the Navy Washington, D. C. 20360 Attn: Code 310C (H. Rosenwasser)	1

	No. Copies
Defense Documentation Center Building 5, Cameron Station Alexandria, Virginia 22314	12
U. S. Army Research Office P.O. Box 12211 Research Triangle Park, N.C. 27709 Attn: CRD-AA-IP	
Commander Naval Undersea Research & Development Ctr. San Diego, California 93132 Attn: Technical Library, Code 133	1
Naval Weapons Center China Lake, California 93555 Attn: Head, Chemistry Div.	1
Naval Civil Engineering Lab Port Hueneme, California 93041 Attn: Mr. W. S. Haynes	1
Professor O. Heinz Dept of Physics & Chemistry Naval Postgraduate School Monterey, California 93940	
Dr. A. L. Slafkosky Scientific Advisor Commandant of the Marine Corps (Code RD-1) Washington, D. C. 20380	1
Dr. Stephen H. Carr Dept of Materials Science Northwestern University Evanston, Illinois 60201	1
Dr. M. Broadhurst Bulk Properties Section National Bureau of Standards U.S. Dept of Commerce Washington, D.C. 20234	2
Dr. C. H. Wang Department of Chemistry University of Utah Salt Lake City, Utah 84112	1

TECHNICAL REPORT DISTRIBUTION LIST (Cont'd)

	No. Copies
Dr. T. A. Litovitz Department of Physics Catholic Univ. of America Washington, D.C. 20017	1
Dr. R. V. Submaranian Washington State Univ. Dept of Materials Science Pullman, Washington 99103	1
Dr. M. Shen Dept of Chemical Engineering Univ. of California Berkeley, California 94720	1
Dr. R. S. Porter Polymer Research Institute and Polymer Science and Engineering University of Massachusetts Amherst, Mass. 01002	1
Dr. H. Freiser Department of Chemistry University of Arizona Tuscon, Arizona 85721	
Dr. V. Stannett Dept of Chemical Engineering North Carolina State University Raleigh, N. C. 27607	1
Dr. D. R. Uhlman Dept of Metallurgy & Material Science Center for Materials Science and Engineering Massachusetts Inst. of Tech. Cambridge, Mass. 02139	1
Naval Surface Weapons Center White Oak Silver Spring, Maryland 20910 Attn: Dr. J. M. Augl Dr. B. Hartmann	1
Dr. G. Goodman Globe Union Inc. 5757 North Green Bay Ave. Milwaukee, Wisconsin 53201	1
Picatinny Arsenal SMUPA-FR-M-D Dover, N. J. 07801 Attn: A. M. Anzalone Bldg. 3401	1

	No. Copies
Dr. J. K. Gillham Princeton University Dept of Chemistry Princeton, N. J. 08540	1
Douglas Aircraft Co. 3855 Lakewood Boulevard Long Beach, California 90846 Attn: Technical Library Cl 290/36-84 AUTO-Sutton	1
Dr. E. Baer Dept of Macromolecular Science Case Western Reserve University Cleveland, Ohio 44106	
Dr. K. D. Pae Dept of Mechanics and Materials Science Rutgers University New Brunswick, New Jersey 08903	1
NASA-Lewis Research Center 21000 Brookpark Road Cleveland, Ohio 44135 Attn: Dr. T. T. Serofini, MS-49-1	1
Dr. Charles H. Sherman, Code TD 121 Naval Underwater Systems Center New London, Connecticut	1
Dr. Alan Gent Department of Physics University of Akron Akron, Ohio 44304	
Mr. Robert W. Jones Advanced Projects Manager Hughes Aircraft Company Mail Station D 132 Culver City, California 90230	1
Dr. C. Giori IIT Research Institute 10 West 35 Street Chicago, Illinois 60616	1
Dr. David Roylance Dept of Materials Sci. and Engin. Massachusetts Inst. of Tech. Cambridge, Massachusetts 02039	1

TECHNICAL REPORT DISTRIBUTION LIST (Cont'd)

	No. Copies
Dr. W. A. Spitzig U.S. Steel Corporation Research Laboratory Monroeville, Penna. 15146	1
Dr. T. P. Conlon, Jr., Code 3622 Sandia Laboratories Sandia Corporation Albuquerque, New Mexico 87115	1
Dr. Martin Kaufmann, Head Materials Res. Branch, Code 4542 Naval Weapons Center China Lake, California 93555	1
Dr. D. A. Vroom Intelcom Rad Tech. P.O. Box 80817 San Diego, California 92138	1
Dr. P. R. Antoniewicz University of Texas Dept of Physics Austin, Texas 78712	1
Dr. W. D. McCormick University of Texas Dept of Physics Austin, Texas 78712	1
Dr. G. A. Somorjai University of California Department of Chemistry Berkeley, California 94720	1
Dr. L. N. Jarvis Surface Chemistry Division 4555 Overlook Ave., S.W. Washington, D. C. 20375	1
Dr. Bruce Wagner, Jr. Northwestern University Materials Research Center Evanston, Illinois 60201	1
Dr. M. H. Chisholm Chemistry Department Princeton University Princeton, N. J. 08540	1
Dr. J. B. Hudson Rensselaer Polytechnic Inst. Materials Division Troy, N. Y. 12181	1
Dr. John T. Yates National Bureau of Standards Dept of Commerce Surface Chemistry Section Washington, D.C. 20234	1
Dr. Theodore E. Madey Dept of Commerce National Bureau of Standards Surface Chemistry Section Washington, D.C. 20234	1
Dr. J. M. White University of Texas Department of Chemistry Austin, Texas 78712	1
Dr. Keith H. Johnson Massachusetts Inst. of Tech. Dept of Metallurgy and Materials Science Cambridge, Massachusetts 02139	1
Dr. M. S. Wrighton Massachusetts Inst. of Tech. Dept of Chemistry Cambridge, Massachusetts 02139	1
Dr. J. E. Demuth IBM Corp. Thomas J. Watson Research Center P.O. Box 218 Yorktown Heights, N. Y. 10598	1
Dr. C. P. Flynn University of Illinois Department of Physics Urbana, Illinois 61801	1
Dr. W. Kohn Department of Physics University of California (San Diego) La Jolla, California 92037	
Dr. R. L. Park Director, Center of Materials Research University of Maryland College Park, Maryland 20742	1
Dr. W. T. Peria Electrical Engineering Dept University of Minnesota Minneapolis, Minnesota 55455	1

TECHNICAL REPORT DISTRIBUTION LIST (Cont'd)

	No. Copies	No. Copies
Dr. Narkis Tzoar City University of N. Y. Convent Ave. at 138th St. New York, New York 10031	1	
Dr. Chia-wei Woo Northwestern University Dept of Physics Evanston, Illinois 60201	1	
Dr. D. C. Mattis Physics Department Yeshiva University Amsterdam Ave & 185th St. New York, N. Y. 10033	1	
Dr. Leonard Wharton Dept of Chemistry James Franck Institute 5640 Ellis Avenue Chicago, Illinois 60637	1	
Dr. M. G. Lagally Dept of Metallurgical and Mining Engineering University of Wisconsin Madison, Wisconsin 53706	1	
Dr. Robert Gomer Dept of Chemistry James Franck Institute 5640 Ellis Avenue Chicago, Illinois 60637		
Dr. R. F. Wallis Dept of Physics University of California (Irvine) Irvine, California 92664	1	
Dr. R. W. Vaughan California Inst. of Technology Div. of Chem. & Chem. Engin. Pasadena, California 91125	1	